PAFNet: A Real-time Deep Learning Model for the Prediction of Paroxysmal Atrial Fibrillation Onset using Single-lead ECG

Dakun Lai , *Member, IEEE*, Peirong Zheng, Yuchen Jiang and Yuxiang Bu

***Abstract*—This study presents PAFNet, a novel real-time deep learning model designed to predict the onset of paroxysmal atrial fibrillation (PAF) at least 45 minutes in advance using a single-lead electrocardiogram (ECG) signal. Fifty ECG records from the publicly accessible PAF prediction challenge database (AFPDB) were used to extract RR interval sequences for the training of PAFNet, while another thirty ECG records from the MIT-BIH Atrial Fibrillation Database (AFDB) and the MIT-BIH Normal Sinus Rhythm Database (NSRDB) were used for database-level testing. Each RR interval sequence was divided into sliding windows of size 100 and a step of 1, which were used as input data for PAFNet. In total, 56,381 PAF_N-type and 56,900 N-type RR interval segments were extracted. The proposed PAFNet features 5 one-dimensional convolutional layers, forming a light-weighted architecture that can accommodate the size of sliding windows by only altering the input layer. Employing the ten-fold cross-validation method, PAFNet achieved an average sensitivity, specificity, and accuracy of 97.12%, 97.77%, and 97.45%, respectively. The promising results suggest that PAFNet achieves high performance and offers the possibility of providing real-time, accurate, and inexpensive clinical tools to assist clinicians in predicting PAF events.**

***Index Terms*—atrial fibrillation, electrocardiography, deep learning, prediction, single-lead**

I. Introduction

A. AF and Paroxysmal Atrial Fibrillation (PAF)

Atrial fibrillation (AF) is a common sustained arrhythmia in clinical practice and can significantly impair quality of life and increase the risk of serious medical conditions, including stroke and heart attack. The prevalence of AF increases with age[1], therefore, as the aging population problem becomes increasingly prominent, the threat of atrial fibrillation to human health becomes increasingly severe. When AF occurs, the disorganized fibrillation of the atrium will reduce the cardiac output and accelerate the formation of a thrombus, which may cause blood vessel block and further lead to life-threatening diseases such as ischemic stroke[2] and myocardial infarction[3].

To evaluate the risk of AF during different phases and take the intervention and treatment in time, AF is commonly divided into different types. Currently, the AF classification according to the presentation, duration, and spontaneous of AF episodes has become a consensus in authoritative guidelines[4], the corresponding five AF types are: first-diagnosed AF, paroxysmal AF (PAF), persistent AF, long-standing persistent AF, and permanent AF. AF usually manifests as PAF at the beginning, which is defined as the AF that terminates spontaneously or with intervention within 7 days of onset.

There are many ways to manage and treat AF, including drug therapy, implanted medical instruments, and radio-frequency ablation, but all these methods carry potential risks. For example, drug therapy has been shown to be effective in patients with newly diagnosed AF with a treatment success rate of about 50%[5, 6], but in the case of patients with persistent AF, it may not only be less effective but also cause other arrhythmias and even fatal complications. So, to prevent irreversible atrial lesions and prevent the further deterioration of AF, early diagnosis of AF has become particularly important.

B. PAF Prediction Significance and State-of-the-Art

Electrocardiogram (ECG) is a commonly used tool that could assist cardiologists to diagnose AF in clinical practice, the development of accurate predictors based on ECG is important for designing high-performance models. Three types of ECG episodes from both normal and PAF subjects are divided as (A) ECG episode of a normal subject under rest state, (B) ECG episode of a PAF subject when AF doesn't occur, and (C) ECG episode of a PAF subject when AF occurs. Compared with the ECG episode from a normal subject, (B) have occasionally premature beats and subtle changes of RR interval in the ECG episode from PAF subjects when AF doesn't occur, which could be used as predictors of the onset of PAF.

Developing a PAF onset prediction model is significant for several reasons. First, when AF doesn't occur, it's difficult to distinguish the ECG of PAF subjects from that of normal subjects. An automatic PAF onset prediction model could assist clinicians in the risk assessment of patients with PAF. Second, the positive prediction result could suggest patients to receive timely interventions, like drug therapy, which could effectively

This work was supported by the National Natural Science Foundation of China under Grant 61771100. (Corresponding authors: Dakun Lai.)

Dakun Lai, Yuxiang Bu and Yuchen Jiang are with the School of Electronic Science and Engineering, University of Electronic Science and Technology of China, Chengdu 610054, China (e-mail: dklai@uestc.edu.cn; 347586493@qq.com; 1260585449@qq.com).

Peirong Zheng is with the School of Electrical and Electronic Engineering, Nanyang Technological University, 50 Nanyang Avenue, Singapore 639798, Singapore (e-mail: pzheng003@e.ntu.edu.sg).

avoid the deterioration of AF in PAF subjects. Third, during postoperative follow-up of radio-frequency ablation surgery, the model is also helpful for assessing the surgical effect.

In March 2001, the PhysioNet Computing in Cardiology Challenge 2001 was held[7], during which researchers proposed various methods to predict the onset of PAF, such as methods based on heart rate variability (HRV)[8-12], atrial premature contraction numbers[13, 14] and P-wave morphology[15]. The publicly accessible PAF prediction challenge database (AFPDB) was also provided in this competition, which could be used to train and test the classification model.

In the last decade, many PAF onset prediction algorithms based on machine learning methods have been proposed, with most of these studies based on the AFPDB. For instance, Mohebbi et al.[16] extracted spectrum, bispectrum and non-linear features from the 30-minute HRV signal and used a support vector machine (SVM)-based classifier to predict the onset of PAF, achieving a sensitivity of 96.3%. Boon et al.[17] used genetic algorithm to optimize the features extracted from 15 minutes HRV signal and also used SVM classifier to predict the onset of PAF, achieving an accuracy of 79.3%. In another study, they used a shorter 5-minute HRV signal and achieved an accuracy of 87.7% [18]. Narin et al.[19] also used 5 minutes HRV signal for the linear and non-linear features extraction, they used the k-nearest neighbors (KNN) classifier and further discussed the performance of the model for data segments in different time windows. Wang et al.[20] improved the speed of SVM algorithm and gained 92.5% accuracy for the test set of different databases but the required length of the signal was 5 minutes long and the generalization ability (87.0% accuracy) on clinical tests was unsatisfying. Sutton et al.[21] proposed the PhysOnline, an open-source streaming physiological signal analysis platform, and demonstrated the effective online prediction of PAF. More recently, many studies have focused on developing AF detection algorithms using deep learning methods[22-26], showing better performance compared with feature extraction[27-29] and machine learning methods[30-32]. However there is a lack of research on the topic of PAF prediction based on deep learning methods.

C. Current Technology Limitations and Study Aims

This study proposes PAFNet, a deep learning model for real-time automatic prediction of the PAF onset based on RR interval sequences derived from single-lead ECG using sliding window technique. PAFNet utilizes ECG information more effectively than existing models that rely solely on hand-crafted features extracted from HRV signals. This approach avoids the loss of important ECG information, which can improve the accuracy of PAF prediction to some extent. Furthermore, instead of traditional machine learning classifiers, we employed a 26-layer lightweight convolutional neural network (CNN) model to improve the performance of PAF prediction, the training of PAFNet is also based on the commonly used AFPDB.

Our study examined PAFNet's performance in terms of sensitivity, specificity, and accuracy. Our model could achieve high accuracy and generalization ability while realizing real-time analysis and prediction. This feature potentially makes PAFNet a useful tool to assist clinicians in evaluating the risk of PAF attacks.

TABLE I

Database		Number of Records (n)	Number of RR intervals (n)
Training and validation	AFPDB (PAF_N)	25	56381
	AFPDB (N)	25	56900
Testing	AFDB (PAF_N)	12	27836
	NSRDB (N)	18	44087

II. Materials and Methods

A. Databases

Table 1 shows that we used AFPDB for training and validating PAFNet, while the MIT-BIH Atrial Fibrillation Database (AFDB) and the MIT-BIH Normal Sinus Rhythm Database (NSRDB) were used to test the model's performance and generalization ability. These publicly accessible databases are available from PhysioNet[33] and contain two ECG channels each. As all channels were collected simultaneously and possess the same RR interval information, we used only single-lead ECG to derive the RR interval sequence.

Fig. 1 (A) shows the learning set of AFPDB, which contains three types of labeled ECG records: PAF normal (PAF_N) type, which is at least 45 minutes away from any AF episodes; PAF onset (PAF_O) type, which is just near the onset of AF; and normal (N) type, with each record lasting 30 minutes. To predict the onset of PAF at least 45 minutes in advance, we used 25 PAF_N-type ECG records and 25 N-type ECG records.

For the test databases, AFDB includes 25 long-term ECG records from subjects with AF (mostly PAF), and NSRDB includes 18 long-term ECG records from subjects with no significant arrhythmia. We extracted PAF_N-type records from AFDB using the same protocol as AFPDB, excluding AF segments less than 5 minutes, atrial flutter segments, and atrial ventricular junction rhythm segments. As a result, we extracted 12 PAF_N-type ECG records and 18 N-type ECG records from these two databases, with each record lasting 30 minutes.

B. ECG Pre-processing and Segmentation

Pre-processing of ECG records through filtering is crucial for improving signal quality and R-wave location accuracy. To reduce different types of noise interferences, we adopted a series of digital filters. First, we used a band-pass filter with a cutoff frequency of 0.1 Hz to 100 Hz to filter out noise beyond the useful frequency range. Next, we removed the baseline drift using a median filter with a window size set to 0.85 of the sampling frequencies. Finally, we used a fourth-order low-pass filter to further eliminate high-frequency noise.

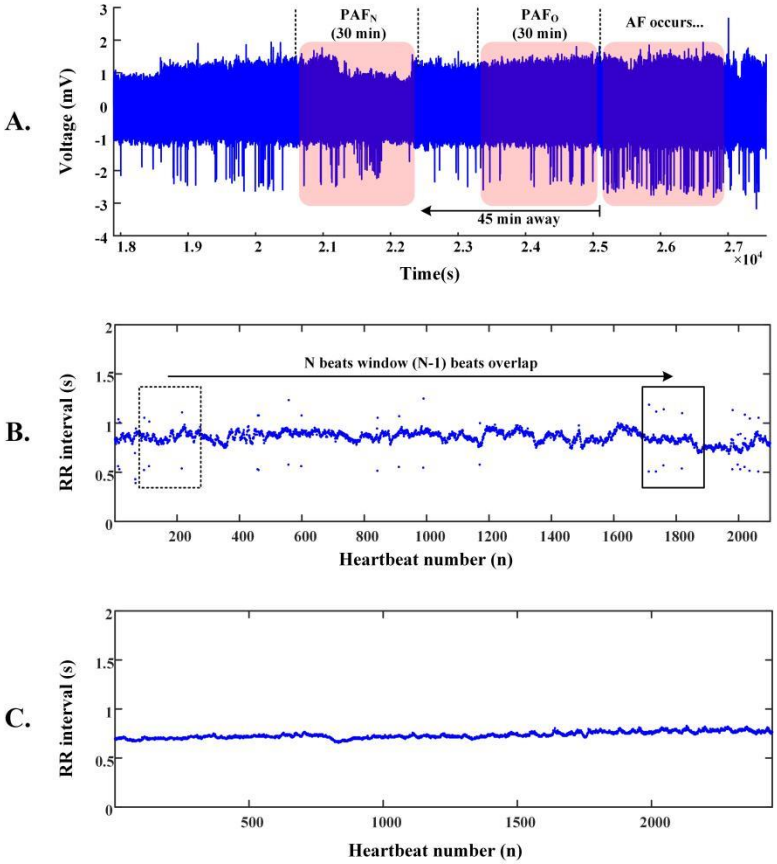

Fig. 1. Demonstration of the data segmentation used for training PAFNet. (A) Two types of 30-minute ECG records before the onset of AF are shown: PAF normal (PAF_N) type, which is at least 45 minutes away from any AF episodes, and PAF onset (PAF_O) type, which is just before the onset of AF. (B) An example of the RR interval sequence derived from a PAF_N record and the corresponding data segmentation based on the sliding window technique. (C) An example of the RR interval sequence derived from a normal sinus record.

Fig. 1 (B) and (C) demonstrate the data segmentation procedure. The RR interval sequence of PAF_N subjects is more fluctuant than that of normal subjects. After pre-processing, we accurately located the R-waves of each ECG record using the difference threshold algorithm, and derived the RR interval sequence using this equation:

$$RR_i = R_{i+1} - R_i \quad (1)$$

RR_i represents the value of the i-th RR interval, R_i represents the time index of the i-th R-wave, and the index i ranges from 1 to M when the ECG record contains (M+1) R-waves.

We then adopted a sliding window with a size of N on each RR interval sequence. This window continuously moved from one side to another, and derived a segment containing N RR intervals during each move. The sliding step could be adjusted according to different application scenarios. In this study, we set the sliding step to 1 to meet the real-time processing requirements and the massive amount of data required for training deep learning models. With a sliding step of 1, we derived (M-N+1) RR interval segments from the whole RR interval sequence.

C. PAFNet

In this study, we explored a real-time and accurate method for predicting the onset of PAF at least 45 minutes in advance by developing a 1D CNN model. Unlike methods that rely on manually extracted HRV features and traditional machine learning classifiers, end-to-end deep learning techniques avoid the need for hand-crafted feature extraction, thus reducing the loss of ECG information and the limitations of prior knowledge. Among these techniques, CNN is well-suited for image processing and automatic feature extraction, making it ideal for image classification and identification[34]. Similarly, the ECG signal and RR interval sequence contain abundant overall and partial information that can be automatically extracted using CNN to identify specific diseases. The CNN model can extract high-level feature maps from 1D signals, enabling accurate identification of specific patterns related to the onset of PAF.

As shown in Fig. 2, PAFNet consisted of 26 layers, including 5 convolutional layers. The input size is the same as the sliding window, with each sample represented by a matrix of one row and N columns, where the column number is the index of the RR interval, and the value is the corresponding RR interval duration in seconds. The 1D convolutional layer, batch normalization layer, activation layer, and 1D maximum pooling layer were abstracted as a block, CBAP layer. The convolutional layer automatically extracted feature maps using kernel techniques, while the batch normalization layer accelerated training and improved accuracy. The activation layer increased the non-linearity of the model, and the pooling layer reduced the scale of the feature map. The flatten layer converted all feature maps into one row as input to the dense layer for the final prediction. The output represents the binary prediction result of PAFNet.

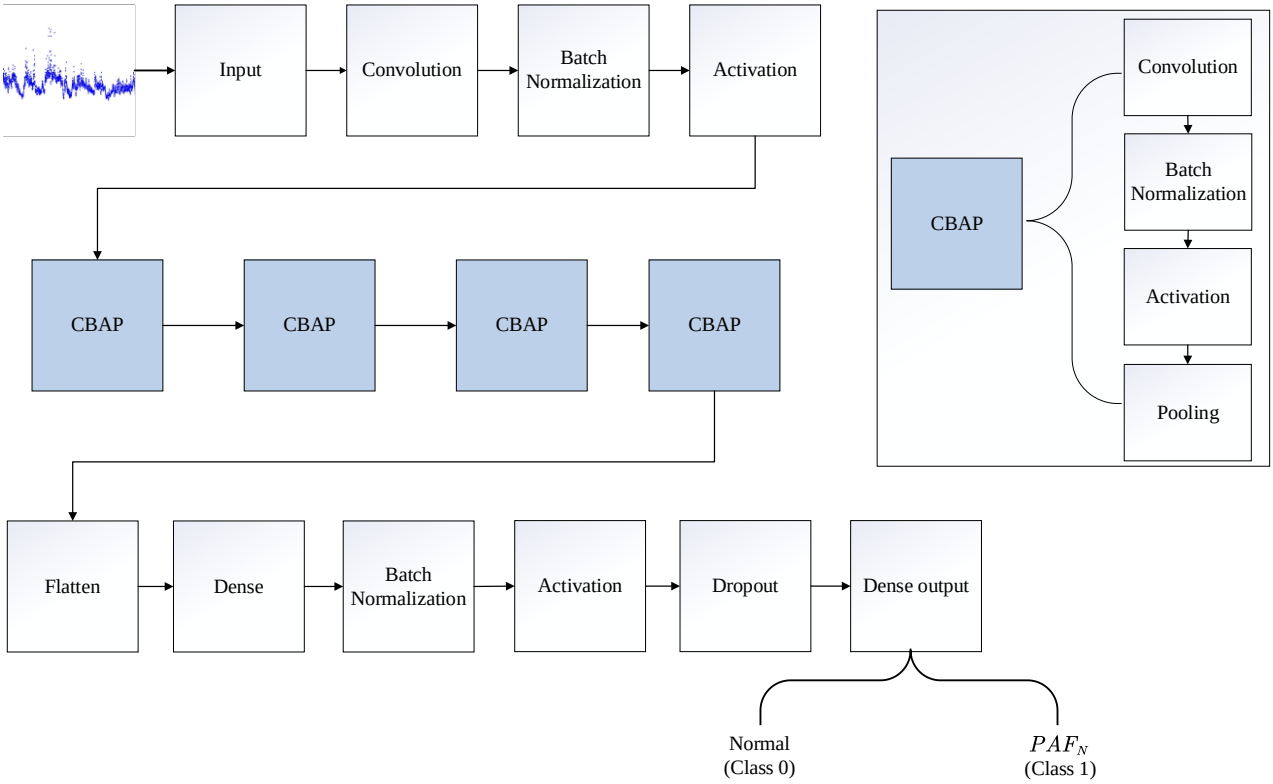

Fig. 2. Illustration of the model structure of PAFNet. The 1D convolutional layer, batch normalization layer, activation layer and 1D max pooling layer are abstracted as CBAP layer.

TABLE II
THE ARCHITECTURE OF PAFNET

Number	Layer type	Number of feature maps or nodes	Parameters	Number	Layer type	Number of feature maps or nodes	Parameters
1	input	changing with the size of the sliding window	N	14	BN	-	-
2	convolutional	16	size: N, kernel: 8, padding="same"	15	activation	-	ReLU
3	BN	-	-	16	pooling	-	size: 2
4	activation	-	ReLU	17	convolutional	256	size: N/16, kernel: 8, padding="same"
5	convolutional	32	size: N/2, kernel: 8, padding="same"	18	BN	-	-
6	BN	-	-	19	activation	-	ReLU
7	activation	-	ReLU	20	pooling	-	size: 2
8	pooling	-	size: 2	21	Flatten	-	-
9	convolutional	64	size: N/4, kernel: 8, padding="same"	22	Dense	512	-
10	BN	-	-	23	BN	-	-
11	activation	-	ReLU	24	activation	-	ReLU
12	pooling	-	size: 2	25	dropout	-	0.25
13	convolutional	128	size: N/8, kernel: 8, padding="same"	26	Dense output	1	activation function: Sigmoid

BN = Batch Normalization

Table II displays the details of the PAFNet's architecture, including hyperparameters and activation functions used. The size of the input layer depends on the size of the sliding window, and the size of the output layer is set to 1, which represents the probability that the corresponding sample is PAF_N. For the CBAP layer, a convolutional kernel size of 100 and a stride of 16 were selected, and the padding method was set to 'valid'. The ReLU function was used as the activation function. A pooling

kernel size of 2 and a stride of 2 were selected to halve the scale of each feature map. The number of output feature maps was set to 16, 32, 64, and 128 for the four CBAP layers, respectively. The size of the flatten layer also depends on the size of the sliding window, and the node number of the first dense layer is set to 2048. A dropout ratio of 0.5 was used to randomly deactivate half of the nodes during each iteration. The training epoch was set to 9, and the batch size was set to 512.

After determining the model's structure, the next step was to optimize the size of the sliding window. Three types of evaluation metrics were used to assess the model's performance with different input sizes, including testing time per batch. A small input size may result in decreased performance due to insufficient ECG information captured by the sliding window, while a larger input size includes more details but may require more testing time per batch.

D. Evaluation Protocols

The limited total sample number of the databases necessitated the use of a stratified ten-fold cross-validation strategy to optimize and evaluate the performance of the PAFNet model during the training and testing procedures. The training dataset, with a sliding window size of 100, yielded 113281 RR interval segments, consisting of 56381 PAF_N type and 56900 N type RR interval segments. To train PAFNet, all segments were randomly divided into ten parts, with nine parts used for training and one part used for validation. This resulted in ten CNN models being trained and saved, with the prediction result of PAFNet during the database level testing procedure obtained by averaging the prediction result of these models. The model's performance was evaluated using the receiver operator characteristic (ROC) curve, which compared the prediction results obtained when using samples of different spans before the onset of PAF as input.

The ability of PAFNet to predict the onset of PAF was evaluated quantitatively using sensitivity (Sen), specificity (Spe), and accuracy (Acc). The total number of true positive (TP), false negative (FN), true negative (TN), and false positive (FP) were counted for PAF_N type as positive and N type as negative, and Sen, Spe, and Acc were calculated based on these statistical parameters.

Finally, based on these statistical parameters, Sen, Spe and Acc were calculated as follows:

$$Sen = \frac{TP}{TP + FN} \tag{2}$$

$$Spe = \frac{TN}{TN + FP} \tag{3}$$

$$Acc = \frac{TP + TN}{TP + FN + TN + FP} \tag{4}$$

III. Results

In this study, the training and testing of the PAFNet model were conducted using the TensorFlow 2.3.0 deep learning framework on a desktop computer equipped with an Intel(R)Core(TM)i9-10900KF CPU@3.70GHz and 64 GB memory. To accelerate processing and reduce training and testing time, an NVIDIA GeForce RTX 3080 GPU with 10 GB memory was also utilized.

Table III summarizes the results of the model input size optimization, where three models were trained using input sizes of 50, 100, and 200 RR intervals, denoted as M1, M2, and M3, respectively. The testing results of these models showed that M2 achieved the highest Sen, Spe, and Acc, with values of 89.92%, 93.24%, and 91.96%, respectively. Notably, M2 exhibited a 4% increase in Sen and nearly 1% increase in Spe compared to M1 and M3. Accordingly, the Acc of M2 increased by nearly 2%, indicating an overall improvement in the model performance. In terms of testing time, M2 was the most efficient, taking only 9.3 milliseconds to process one input sample, whereas M1 and M3 took 13.8 milliseconds and nearly 30 milliseconds, respectively, to process a batch of data (i.e., 512 samples). Based on these results, the input size of 100 was selected, and M2 was identified as the optimized model.

Table IV presents the results of ten-fold cross-validation of the PAFNet model using 100 RR intervals as input (M2 in Table III). The sliding window size is set to 100, with a sliding step of 1 as mentioned in section 2. During the ten-fold cross-validation, the 113281 training and validation samples are randomly shuffled and divided into 10 parts, with each part

TABLE III
MODEL INPUT SIZE OPTIMIZATION

Model	Input size (n)	Sen (%)	Spe (%)	Acc (%)	Testing time (ms / batch)
M1	50	85.44	92.45	89.74	13.8
M2	**100**	**89.92**	**93.24**	**91.96**	**23.1**
M3	200	88.17	93.47	91.42	43.0

TABLE IV
TEN-FOLD CROSS VALIDATION USING 100 RR INTERVALS OVERLAPPED WINDOW AS INPUT

Fold	Training data (rows)	Validation data (rows)	Sen (%)	Spe (%)	Acc (%)
1	11329-113281	1-11328	82.11	92.09	87.16
2	1-11328, 22656-113281	11328-22656	95.34	87.84	91.63
3	1-22656, 33984-113281	22656-33984	98.74	98.86	98.80
4	1-33984, 45312-113281	33984-45312	99.39	99.39	99.39
5	1-45312, 56640-113281	45312-56640	100.00	100.00	100.00
6	1-56640, 67968-113281	56640-67968	98.76	99.95	99.35
7	1-67968, 79296-113281	67968-79296	100.00	100.00	100.00
8	1-79296, 90624-113281	79296-90624	98.47	100.00	99.21
9	1-90624, 101952-113281	90624-101952	98.43	99.54	98.98
10	1-101952	101952-113281	100.00	100.00	100.00
Mean	-	-	**97.12**	**97.77**	**97.45**
Var			0.0030	0.0018	0.0019

Var = variance

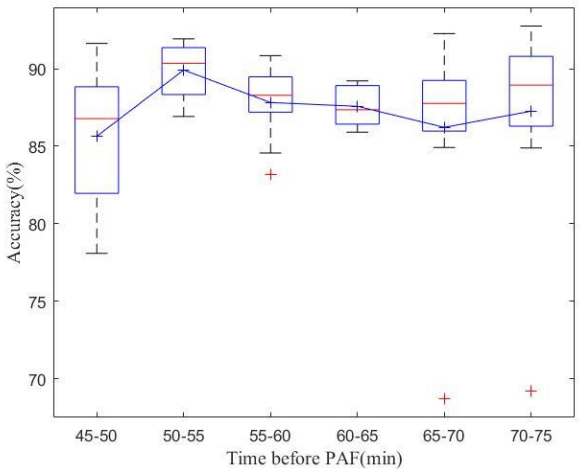

Fig. 3. Comparison of the model classification accuracy using the ECG signals in different time periods before the onset of AF as the input data of PAFNet.

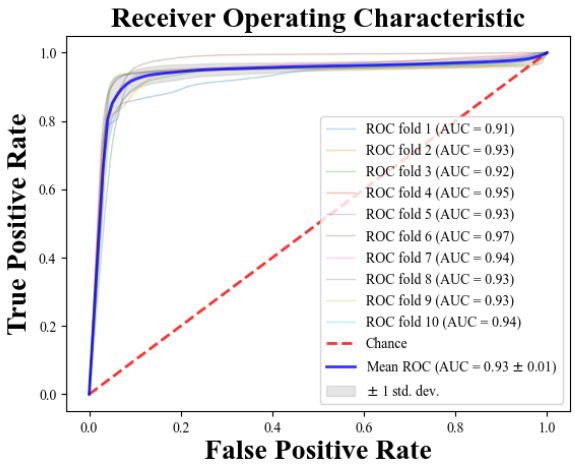

Fig. 4. Receiver operating characteristic (ROC) curves of the ten folds during model test.

used once for validation and nine times for training. The fifth and seventh fold show the highest accuracy of 100.00%, while the first fold shows the lowest accuracy of 87.16%, indicating significant variability. Notably, the validation results are substantially higher than the testing results of Sen, Spe, and Acc for M2 in Table III, at 97.12%, 97.77%, and 97.45%, respectively.

Fig. 3 and Fig. 4 present the results of the database-level testing, which aimed to evaluate the generalization ability of the model using different databases. Fig. 3 shows the prediction accuracy of PAFNet using input samples of different spans before the onset of PAF. The horizontal axis represents the different spans, which started at 75 minutes before the PAF onset, while the vertical axis represents the prediction accuracy. The resultant curve indicates that the accuracy fluctuates around 85% and does not significantly change when the span of the sample varies. Fig. 4 depicts the receiver operator characteristic (ROC) curves of the ten models during the ten folds of the stratified ten-fold cross-validation. The bold blue curve denotes the ROC curve of the average prediction results. The proposed PAFNet achieved high performance for both positive and negative samples, and the mean area under the curve (AUC) was about 0.93, with AUC values ranging from 0.91 to 0.97 in each fold.

IV. Discussion

A. Real-time PAF Onset Prediction

The HRV analysis was commonly used in studies on the topic of PAF prediction, the extracted HRV features including time domain, frequency, nonlinear and time-frequency domain features could reflect the variability of RR intervals and indirectly reflect the influence of premature beats and other heart rhythms. This kind of method have a relatively mature theoretical system and implementation, and could be well compatible with the feature selection methods and machine learning classifiers, but the time duration of the ECG signal used for HRV analysis is at least 5 minutes which doesn't meet the requirements of the real-time monitoring scenarios[35].

Unlike the HRV analysis, we proposed a real-time PAF onset prediction method based on the raw RR interval sequence and sliding window technique, which effectively solves the problem of poor real-time performance in traditional PAF prediction methods. Compared with the commonly used HRV analysis, which requires at least a 5-minute ECG signal, our method allows for real-time monitoring scenarios such as ICU PAF monitoring. The sliding window technique enables the capture of RR intervals in a fixed number as the window moves on the RR interval sequence, updating with each new R wave detected by the R wave location algorithm. The highly effective PAF prediction algorithm, which processes one sample in only 23.1 milliseconds, allows for the whole system to make a new prediction with each new heartbeat, meeting the requirements of real-time PAF onset prediction scenarios. This method offers a promising approach for real-time PAF prediction, with potential for further development and application in clinical settings.

B. Performance Compared with Other Methods

Our proposed method for predicting PAF offers several advantages, including the use of deep learning to improve prediction accuracy. We used the CNN technique to achieve end-to-end prediction and classification, with raw RR interval segments as input samples to preserve ECG information. PAF prediction requires longer ECG signals than AF detection or classification, as shown in Table III. When the input size was set to 50 (approximately 30-50 seconds ECG signal), the prediction accuracy was 89.74%. Increasing the input size to 100 didn't significantly improve accuracy, which was 91.42%, approximately equal to the accuracy achieved with an input size of 200. However, increasing the input size results in a smaller total number of samples, which is why deep learning is rarely used in related studies. To address this issue, we adopted a sliding window with a step of 1 RR interval, generating a sufficient training database. Using this methodology, we achieved high accuracy in predicting PAF and demonstrated the effectiveness of our approach.

Table V shows the benchmarking results of our proposed method against other previous studies. Our PAFNet performed better than most studies using machine learning methods. These studies used input sizes varying from 5 to 30 minutes to extract different HRV features and employed classifiers such as SVM

TABLE V
THE COMPARISON BETWEEN THE PROPOSED METHOD AND PREVIOUS STUDIES

Author (year)	Methodology			Validation (and Test) Performance		
	Input size	Features extraction	Classifier	Sen (%)	Spe (%)	Acc (%)
Mohebbi (2012)[16]	30 minutes	14 HRV frequency domain and nonlinear features	SVM	96.30	93.10	94.50
Boon (2016)[17]	15 minutes	55 HRV features	SVM	77.40	81.10	79.30
Boon[18] (2018)	5 minutes	53 HRV time domain, frequency domain, and nonlinear features	SVM	86.80	88.70	87.70
Narin[19] (2018)	5 minutes	26 HRV time domain and frequency domain features	KNN	92.00	88.00	90.00
Wang[20] (2021)	5 minutes	P wave and RR intervals	IQPSO-SVM	93.30 (94.20)	91.70 (79.70)	92.50 (87.00)
Present study	100 RR intervals (Approximately 1.5 minutes)	RR intervals	CNN	97.77 (89.92)	97.12 (93.24)	97.45 (91.96)

and KNN to predict PAF. Compared to these studies, our proposed PAFNet achieved higher Sen, Spe, and Acc than studies using input sizes of 5 and 15 minutes[17-19]. However, the study by Mohebbi et al.[16] showed better performance than ours, likely due to their use of the whole 30 minutes ECG from each record, which sacrificed real-time performance for improved prediction accuracy. Additionally, their studies didn't conduct database-level tests. Wang et al.[20] developed models with competitive performance on testing, but their model requires a 5-minute input and hand-crafted P wave, which is significantly longer than the input length required for our proposed method. Overall, our proposed PAFNet demonstrates the effectiveness of deep learning approach, outperforming most previous studies using machine learning methods.

C. Limitations and Future Works

Although this study proposed a real-time PAF prediction model that outperformed many previous studies, there are still some limitations. Firstly, while the total number of samples is large, the number of records in the training database is limited, resulting in insufficient variation in the ECG signals. This may explain why the generalization ability of PAFNet was not excellent during the database-level testing. As the testing subjects differ from those in AFPDB, the database-level testing serves as a small-scale clinical validation. As shown in Fig. 3, the average Sen, Spe, and Acc during the testing procedure were 89.92%, 93.24%, and 91.96%, respectively, indicating that the generalization ability of PAFNet needs to be further improved. Secondly, all the programs were deployed on a desktop computer with an efficient GPU in this study. Future studies could focus on hardware implementation to test the real-time performance of the model on embedded systems with limited resources and processing performance. Making PAFNet lighter could be achieved by reducing the number of blocks, the size of the sliding window, and increasing the step length. These limitations highlight opportunities for further research to improve the performance and applicability of the PAF prediction model.

V. CONCLUSION

The ability to predict PAF at least 45 minutes in advance can help clinicians assess the risk of PAF events and provide timely intervention for patients. However, previous PAF prediction studies based on HRV analysis and traditional machine learning methods have had limitations such as unsatisfactory real-time processing speed and prediction performance. This study proposes PAFNet, a real-time deep learning model that uses sliding window and CNN techniques to achieve high-performance PAF prediction. The model requires only a single-lead ECG signal as input to extract the RR interval sequence, making it suitable for clinical application even in scenarios with limited medical resources and conditions. Our results suggest that the customized 26-layer CNN, with five weighted layers paired with a sliding window of length 100 RR intervals, can achieve relatively high performance and may offer a real-time, accurate, and inexpensive clinical tool for predicting PAF events. In conclusion, PAFNet provides a promising approach to improve PAF prediction and has the potential to be a valuable tool for clinicians in identifying and treating PAF events.

ACKNOWLEDGMENT

This work was supported by the National Natural Science Foundation of China under Grant 61771100. The authors would like to thank Biomedical Imaging and Electrophysiology Laboratory (BMI-EP), University of Electronic Science and Technology of China for providing computational and biomedical equipment.

REFERENCES

[1] S. Colilla, A. Crow, W. Petkun, D. E. Singer, T. Simon, and X. C. Liu, "Estimates of Current and Future Incidence and Prevalence of Atrial Fibrillation in the US Adult Population," (in English), *Am J Cardiol,* vol. 112, no. 8, pp. 1142-1147, Oct 15 2013, doi: 10.1016/j.amjcard.2013.05.063.

[2] C. E. Chiang *et al.*, "2017 consensus of the Asia Pacific Heart Rhythm Society on stroke prevention in atrial fibrillation," *J Arrhythm,* vol. 33, no. 4, pp. 345-367, Aug 2017, doi: 10.1016/j.joa.2017.05.004.

[3] E. Z. Soliman *et al.*, "Atrial Fibrillation and the Risk of Myocardial Infarction," (in English), *Jama Intern Med,* vol. 174, no. 1, pp. E107-E114, Jan 2014, doi: 10.1001/jamainternmed.2013.11912.

[4] G. Hindricks *et al.*, "2020 ESC Guidelines for the diagnosis and management of atrial fibrillation developed in collaboration with the European Association for Cardio-Thoracic Surgery (EACTS)," *Eur Heart J,* vol. 42, no. 5, pp. 373-498, Feb 1 2021, doi: 10.1093/eurheartj/ehaa612.

[5] W. S. Chen *et al.*, "Comparison of pharmacological and electrical cardioversion in permanent atrial fibrillation after prosthetic cardiac valve replacement: A prospective randomized trial," (in English), *J Int Med Res,* vol. 41, no. 4, pp. 1067-1073, Aug 2013, doi: 10.1177/0300060513489800.

[6] A. K. Gitt, W. Smolka, G. Michailov, A. Bernhardt, D. Pittrow, and T. Lewalter, "Types and outcomes of cardioversion in patients admitted to hospital for atrial fibrillation: results of the German RHYTHM-AF Study," (in English), *Clin Res Cardiol,* vol. 102, no. 10, pp. 713-723, Oct 2013, doi: 10.1007/s00392-013-0586-x.

[7] G. B. Moody, A. L. Goldberger, S. McClennen, and S. P. Swiryn, "Predicting the onset of paroxysmal atrial fibrillation: The Computers in Cardiology Challenge 2001," presented at the Computers in Cardiology, Rotterdam, Netherlands, 2001. [Online]. Available: <Go to ISI>://WOS:000173806400029.

[8] P. de Chazal and C. Heneghan, "Automated assessment of atrial fibrillation," presented at the Computers in Cardiology 2001, Rotterdam, Netherlands, 2001. [Online]. Available: <Go to ISI>://WOS:000173806400030.

[9] K. S. Lynn and H. D. Chiang, "A two-stage solution algorithm for paroxysmal atrial fibrillation prediction," presented at the Computers in Cardiology 2001, Rotterdam, Netherlands, 2001. [Online]. Available: <Go to ISI>://WOS:000173806400103.

[10] G. Krstacic, D. Gamberger, T. Smuc, and A. Krstacic, "Some important R-R interval based paroxysmal atrial fibrillation predictors," presented at the Computers in Cardiology 2001, Rotterdam, Netherlands, 2001. [Online]. Available: <Go to ISI>://WOS:000173806400104.

[11] C. Maier, M. Bauch, and H. Dickhaus, "Screening and prediction of paroxysmal atrial fibrillation by analysis of heart rate variability parameters," presented at the Computers in Cardiology 2001, Rotterdam, Netherlands, 2001. [Online]. Available: <Go to ISI>://WOS:000173806400033.

[12] A. C. C. Yang and H. W. Yin, "Prediction of paroxysmal atrial fibrillation by footprint analysis," presented at the Computers in Cardiology 2001, Rotterdam, Netherlands, 2001. [Online]. Available: <Go to ISI>://WOS:000173806400102.

[13] P. Langley *et al.*, "Can paroxysmal atrial fibrillation be predicted?," presented at the Computers in Cardiology 2001, Rotterdam, Netherlands, 2001. [Online]. Available: <Go to ISI>://WOS:000173806400031.

[14] W. Zong, R. Mukkamala, and R. G. Mark, "A methodology for predicting paroxysmal atrial fibrillation based on ECG arrhythmia feature analysis," presented at the Computers in Cardiology 2001, Rotterdam, Netherlands, 2001. [Online]. Available: <Go to ISI>://WOS:000173806400032.

[15] G. Schreier, P. Kastner, and W. Marko, "An automatic ECG processing algorithm to identify patients prone to paroxysmal atrial fibrillation," presented at the Computers in Cardiology 2001, Rotterdam, Netherlands, 2001. [Online]. Available: <Go to ISI>://WOS:000173806400034.

[16] M. Mohebbi and H. Ghassemian, "Prediction of paroxysmal atrial fibrillation based on non-linear analysis and spectrum and bispectrum features of the heart rate variability signal," (in English), *Comput Meth Prog Bio,* vol. 105, no. 1, pp. 40-49, Jan 2012, doi: 10.1016/j.cmpb.2010.07.011.

[17] K. H. Boon, M. Khalil-Hani, M. B. Malarvili, and C. W. Sia, "Paroxysmal atrial fibrillation prediction method with shorter HRV sequences," (in English), *Comput Meth Prog Bio,* vol. 134, pp. 187-196, Oct 2016, doi: 10.1016/j.cmpb.2016.07.016.

[18] K. H. Boon, M. Khalil-Hani, and M. B. Malarvili, "Paroxysmal atrial fibrillation prediction based on HRV analysis and non-dominated sorting genetic algorithm III," (in English), *Comput Meth Prog Bio,* vol. 153, pp. 171-184, Jan 2018, doi: 10.1016/j.cmpb.2017.10.012.

[19] A. Narin, Y. Isler, M. Ozer, and M. Perc, "Early prediction of paroxysmal atrial fibrillation based on short-term heart rate variability," (in English), *Physica A,* vol. 509, pp. 56-65, Nov 1 2018, doi: 10.1016/j.physa.2018.06.022.

[20] L. H. Wang *et al.*, "A Classification and Prediction Hybrid Model Construction with the IQPSO-SVM Algorithm for Atrial Fibrillation Arrhythmia," *Sensors (Basel),* vol. 21, no. 15, Aug 1 2021, doi: 10.3390/s21155222.

[21] J. R. Sutton, R. Mahajan, O. Akbilgic, and R. Kamaleswaran, "PhysOnline: An Open Source Machine Learning Pipeline for Real-Time Analysis of Stream Physiological Waveform," (in English), *Ieee J Biomed Health,* vol. 23, no. 1, pp. 59-65, Jan 2019, doi: 10.1109/Jbhi.2018.2832610.

[22] U. R. Acharya, H. Fujita, O. S. Lih, Y. Hagiwara, J. H. Tan, and M. Adam, "Automated detection of arrhythmias using different intervals of tachycardia ECG segments with convolutional neural network," *Information Sciences,* vol. 405, pp. 81-90, Sep 2017, doi: 10.1016/j.ins.2017.04.012.

[23] X. Fan, Q. Yao, Y. Cai, F. Miao, F. Sun, and Y. Li, "Multiscaled Fusion of Deep Convolutional Neural Networks for Screening Atrial Fibrillation From Single Lead Short ECG Recordings," *Ieee J Biomed Health,* vol. 22, no. 6, pp. 1744-1753, Nov 2018, doi: 10.1109/jbhi.2018.2858789.

[24] A. Y. Hannun *et al.*, "Cardiologist-level arrhythmia detection and classification in ambulatory electrocardiograms using a deep neural network," *Nature Medicine,* vol. 25, no. 1, pp. 65-+, Jan 2019, doi: 10.1038/s41591-018-0268-3.

[25] R. Kamaleswaran, R. Mahajan, and O. Akbilgic, "A robust deep convolutional neural network for the classification of abnormal cardiac rhythm using single lead electrocardiograms of variable length," *Physiological Measurement,* vol. 39, no. 3, Mar 2018, Art no. 035006, doi: 10.1088/1361-6579/aaaa9d.

[26] J. Rubin, S. Parvaneh, A. Rahman, B. Conroy, and S. Babaeizadeh, "Densely connected convolutional networks for detection of atrial fibrillation from short single-lead ECG recordings," (in English), *J Electrocardiol,* vol. 51, no. 6, pp. S18-S21, Nov-Dec 2018, doi: 10.1016/j.jelectrocard.2018.08.008.

[27] J. Lian, L. Wang, and D. Muessig, "A Simple Method to Detect Atrial Fibrillation Using RR Intervals," *Am J Cardiol,* vol. 107, no. 10, pp. 1494-1497, May 15 2011, doi: 10.1016/j.amjcard.2011.01.028.

[28] M. Stridh, L. Sornmo, C. J. Meurling, and S. B. Olsson, "Sequential characterization of atrial tachyarrhythmias based on ECG time-frequency analysis," (in English), *Ieee T Bio-Med Eng,* vol. 51, no. 1, pp. 100-114, Jan 2004, doi: 10.1109/Tbme.2003.820331.

[29] E. K. Roonizi and R. Sassi, "An Extended Bayesian Framework for Atrial and Ventricular Activity Separation in Atrial Fibrillation," (in English), *Ieee J Biomed Health,* vol. 21, no. 6, pp. 1573-1580, Nov 2017, doi: 10.1109/Jbhi.2016.2625338.

[30] S. Mehta, N. Lingayat, and S. Sanghvi, "Detection and delineation of P and T waves in 12-lead electrocardiograms," *Expert Systems,* vol. 26, no. 1, pp. 125-143, Feb 2009, doi: 10.1111/j.1468-0394.2008.00486.x.

[31] S. Ladavich, B. Ghoraani, and Ieee, "Developing An Atrial Activity-Based Algorithm For Detection Of Atrial Fibrillation," presented at the 2014 36th Annual International Conference of the Ieee Engineering in Medicine and Biology Society, Chicago, IL, USA, 2014. [Online]. Available: <Go to ISI>://WOS:000350044700014.

[32] A. Kennedy, D. D. Finlay, D. Guldenring, R. R. Bond, K. Moran, and J. McLaughlin, "Automated detection of atrial fibrillation using R-R intervals and multivariate-based classification," *J Electrocardiol,* vol. 49, no. 6, pp. 871-876, Nov-Dec 2016, doi: 10.1016/j.jelectrocard.2016.07.033.

[33] A. L. Goldberger *et al.*, "PhysioBank, PhysioToolkit, and PhysioNet - Components of a new research resource for complex physiologic signals," (in English), *Circulation,* vol. 101, no. 23, pp. E215-E220, Jun 13 2000, doi: DOI 10.1161/01.CIR.101.23.e215.

[34] Y. LeCun, Y. Bengio, and G. Hinton, "Deep learning," *Nature,* vol. 521, no. 7553, pp. 436-444, May 28 2015, doi: 10.1038/nature14539.

[35] A. J. Camm *et al.*, "Heart rate variability - Standards of measurement, physiological interpretation, and clinical use," (in English), *Circulation,* vol. 93, no. 5, pp. 1043-1065, Mar 1 1996, doi: Doi 10.1016/0044-8486(94)90048-5.